Biogeosciences, 14, 1365–1381, 2017
www.biogeosciences.net/14/1365/2017/
doi:10.5194/bg-14-1365-2017

Biogeosciences Open Access EGU

Gas chromatography vs. quantum cascade laser-based N_2O flux measurements using a novel chamber design

Christian Brümmer[1], Bjarne Lyshede[1], Dirk Lempio[1], Jean-Pierre Delorme[1], Jeremy J. Rüffer[1,*], Roland Fuß[1], Antje M. Moffat[1], Miriam Hurkuck[1], Andreas Ibrom[2], Per Ambus[3], Heinz Flessa[1], and Werner L. Kutsch[1,4]

[1]Thünen Institute of Climate-Smart Agriculture, Braunschweig, Germany
[2]Department of Environmental Engineering, Technical University of Denmark, Lyngby, Denmark
[3]Department of Geosciences and Natural Resource Management, University of Copenhagen, Copenhagen, Denmark
[4]Integrated Carbon Observation System, ICOS ERIC Head office, Helsinki, Finland
[*]previously published under the name Jeremy Smith

Correspondence to: Christian Brümmer (christian.bruemmer@thuenen.de)

Received: 28 June 2016 – Discussion started: 6 July 2016
Revised: 22 February 2017 – Accepted: 28 February 2017 – Published: 20 March 2017

Abstract. Recent advances in laser spectrometry offer new opportunities to investigate the soil–atmosphere exchange of nitrous oxide. During two field campaigns conducted at a grassland site and a willow field, we tested the performance of a quantum cascade laser (QCL) connected to a newly developed automated chamber system against a conventional gas chromatography (GC) approach using the same chambers plus an automated gas sampling unit with septum capped vials and subsequent laboratory GC analysis. Through its high precision and time resolution, data of the QCL system were used for quantifying the commonly observed nonlinearity in concentration changes during chamber deployment, making the calculation of exchange fluxes more accurate by the application of exponential models. As expected, the curvature values in the concentration increase was higher during long (60 min) chamber closure times and under high-flux conditions ($F_{N_2O} > 150\,\mu g\ N\,m^{-2}\,h^{-1}$) than those values that were found when chambers were closed for only 10 min and/or when fluxes were in a typical range of 2 to 50 $\mu g\ N\,m^{-2}\,h^{-1}$. Extremely low standard errors of fluxes, i.e., from ∼ 0.2 to 1.7 % of the flux value, were observed regardless of linear or exponential flux calculation when using QCL data. Thus, we recommend reducing chamber closure times to a maximum of 10 min when a fast-response analyzer is available and this type of chamber system is used to keep soil disturbance low and conditions around the chamber plot as natural as possible. Further, applying linear regression to a 3 min data window with rejecting the first 2 min after closure and a sampling time of every 5 s proved to be sufficient for robust flux determination while ensuring that standard errors of N_2O fluxes were still on a relatively low level. Despite low signal-to-noise ratios, GC was still found to be a useful method to determine the mean the soil–atmosphere exchange of N_2O on longer timescales during specific campaigns. Intriguingly, the consistency between GC and QCL-based campaign averages was better under low than under high N_2O efflux conditions, although single flux values were highly scattered during the low efflux campaign. Furthermore, the QCL technology provides a useful tool to accurately investigate the highly debated topic of diurnal courses of N_2O fluxes and its controlling factors. Our new chamber design protects the measurement spot from unintended shading and minimizes disturbance of throughfall, thereby complying with high quality requirements of long-term observation studies and research infrastructures.

1 Introduction

The accurate determination of ambient nitrous oxide (N_2O) concentrations and the associated exchange between soil and atmosphere has been in the focus of environmental research for several years. Nitrous oxide is of high relevance for the Earth's greenhouse gas budget due to its long residence time in the troposphere and its relatively large energy absorption capacity per molecule, resulting in a cumulative radia-

tive forcing almost 300 times higher than the same mass unit of carbon dioxide over a 100-year period when climate–carbon feedbacks are included (IPCC, 2013). It is predominantly emitted as a by-product of nitrification and an intermediate product of denitrification and nitrifier denitrification, which are key microbiological processes in the soil nitrogen (N) cycle (Firestone and Davidson, 1989; Wrage et al., 2001; Thomson et al., 2012; Butterbach-Bahl et al., 2013). Main N_2O sources are agricultural activities in the form of N fertilization. In smaller quantities, N_2O is also produced through biomass burning, degassing of irrigation water, and industrial processes (Seinfeld and Pandis, 2006). On the other hand, some field studies report that soils can also consume N_2O, although the strength of this sink has not yet been thoroughly evaluated (Donoso et al., 1993; IPCC 2007; Chapuis-Lardy et al., 2007).

Precise measurements of N_2O – particularly on the field scale – are therefore essential for specific applications in ecosystem research such as the study of N cycling, fertilization effects, and the compilation of full greenhouse gas budgets. The most common method to measure the soil–atmosphere exchange of N_2O is the operation of static chambers (Hutchinson and Mosier, 1981; Schiller and Hastie, 1996). The N_2O flux is calculated from the concentration increase (or decrease) over time in a gas-tight chamber, which is usually attached to a collar that is permanently inserted into the soil. A number of approaches have emerged over the last years where the air sample is either manually collected using a syringe through a septum and/or directly inserted into sample vials (e.g., Castaldi et al., 2010; Jassal et al., 2008, 2011; Livesley et al., 2011; Lohila et al., 2010; Parkin and Venterea, 2010, and references therein) with subsequent analysis on gas chromatography (GC) systems using ^{63}Ni electron capture detectors for N_2O detection. Different chamber designs and air sampling procedures exist, either with manual, semiautomated (i.e., automatic sampling but manual transport of air samples in syringes or vials to the GC – this study), or fully automated gas collection, where the air samples are directly pumped (or sucked) via carrier gas to a temperature-stable housing equipped with a GC in the field (e.g., Brümmer et al., 2008; Butterbach-Bahl et al., 1997; Dannenmann et al., 2006; Flessa et al., 2002; Papen and Butterbach-Bahl, 1999; Rosenkranz et al., 2006).

In the last decade, substantial progress has been made in the development of fast-response technologies for analyzing a variety of N and carbon (C) trace gases. These are tunable diode laser absorption spectrometers (TDLASs), quantum cascade lasers (QCLs), and devices originating from individual applications such as Fourier transform infrared (FTIR) spectrometers or custom-made converters coupled to chemiluminescence detectors (CLDs). These robust, fast, and precise analyzers are essential for the long-term monitoring of biosphere–atmosphere exchange and have even allowed first eddy covariance (EC) measurements of field-scale N_2O, methane (CH_4) (e.g., Rinne et al., 2005; Denmead et al., 2010; Kroon et al., 2010; Neftel et al., 2010; Tuzson et al., 2010; Jones et al., 2011; Merbold et al., 2014), and reactive N fluxes (Horii et al., 2004; Ammann et al., 2012; Brümmer et al., 2013). Continuous observations of trace gas exchange over timescales from hours to decades enable researchers to evaluate diurnal, seasonal, and interannual variability and trends as well as the elucidation of climatic and management controls on gas exchange patterns (e.g., Baldocchi et al., 2001; Brümmer et al., 2012; Kutsch et al., 2010). With regard to chamber measurements, it is expected that the precision and time resolution of the abovementioned technologies may considerably reduce the chamber closure duration for single flux measurement events, thereby minimizing plot disturbance and allowing for a significant increase in repeated measurements leading to more robust databases, which are required for reliable greenhouse gas budgets. Although the EC methodology provides near-continuous time series of greenhouse gas concentrations and exchange, chamber measurements will certainly still be required in the future as prerequisites for EC measurements are sometimes not fulfilled (for example through insufficient turbulent mixing, complex terrain, inhomogeneous fetch) and small-scale spatial variability or emissions from replicated field plot experiments can only be determined by chamber measurements. Some first examples of high-resolution chamber measurements using fast-response analyzers can be found in Cowan et al. (2014a, b), Hensen et al. (2006), Laville et al. (2011), Sakabe et al. (2015), and Savage et al. (2014).

The comparability, applicability, and uncertainty associated with the respective approach are currently debated in the ecosystem research community, e.g., when comparing fluxes from GC–vial systems with those from more recent continuous setups such as QCL systems. In this context, the flux determination method was found to be an important factor (e.g., Kroon et al., 2008; Forbrich et al., 2010). Fluxes are often calculated using a linear regression of the change in headspace concentration over time and are scaled to the collar area, including a temperature and pressure correction (e.g., Savage et al., 2014). However, several other studies demonstrate the need for nonlinear models for soil–atmosphere trace gas flux estimation (Hutchinson and Mosier, 1981; Livingston et al., 2006; Kutzbach et al., 2007; Kroon et al., 2008; Pedersen et al., 2010; Pihlatie et al., 2013). It has been argued that molecular diffusion theory states that chamber effects lead to declining gradients in the relationship between concentration and time and that slight chamber leakages create the same effect (Hutchinson and Mosier, 1981; Livingston et al., 2006; Pedersen et al., 2010). Nevertheless, linear concentration data often predominate (e.g., Forbrich et al., 2010), which may not necessarily be in conflict with the theory as nonlinearity is sometimes not visible in data series with only a limited number of samples (mostly due to noisy concentration measurements or effects of small chambers; Pedersen et al., 2010).

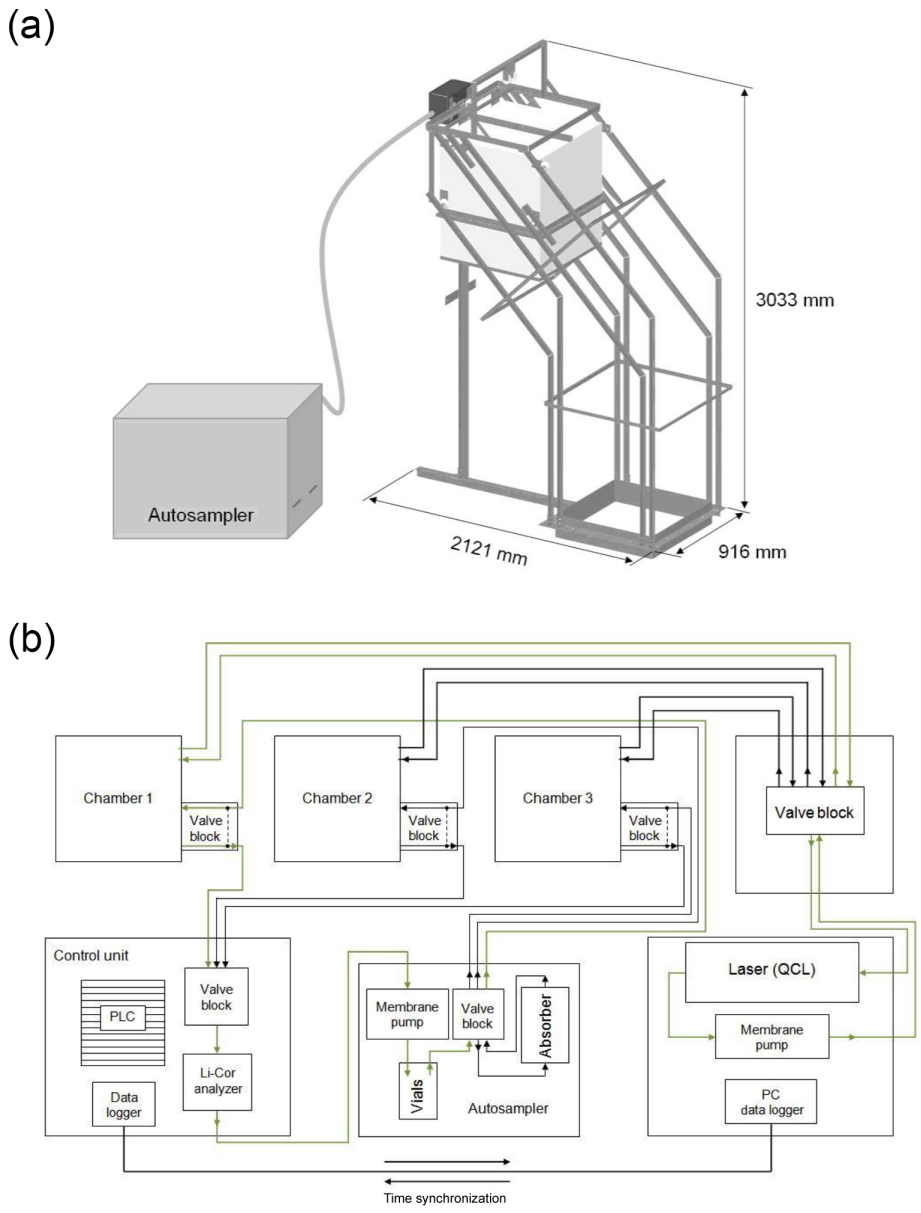

Figure 1. Schematic diagrams of an automated chamber connected to an autosampler unit **(a)** and of the entire chamber system **(b)**. Green lines indicate that Chamber 1 is currently in measurement mode. See text for detailed description.

To further investigate effects of flux estimation methods on the one hand and the use of different gas analyzer types on the other hand, our study comprises N_2O chamber flux measurements from two campaigns conducted with a newly developed chamber system under different environmental conditions. The aims of this study were as follows:

- presentation of a novel chamber design that is connected to both a vial air sampling setup with subsequent GC analysis and a QCL spectrometer
- characterization of the shape of the concentration increase/decrease to identify whether $\partial c/\partial t$ is linear or nonlinear, including a quantification of the curvature (κ) in concentration increase/decrease (Sect. 3.1); the parameter κ was further used to verify chamber sealing by checking its dependency on wind speed, wind direction, the flux itself, and closure time
- comparison of N_2O fluxes and their associated standard errors from linear and nonlinear regression models (Sect. 3.2)
- testing the novel chamber system under high- and low-flux conditions and comparing GC vs. QCL-based flux estimates (Sect. 3.3)

– investigation of ecosystem and climate-specific flux characteristics such as N_2O uptake and diurnal variation (Sect. 3.4).

2 Methods

2.1 Chamber design

Nitrous oxide measurements were carried out using a newly developed semiautomatic chamber system (Fig. 1). It consisted of aluminum guiding racks (length 2121, width 936, height 3033 mm) with aluminum soil collars (length 750, width 750, height 160 mm; inserted 0.10 m into the soil), and opaque PVC chambers (color: white; interior dimensions: length 777, width 777, height 565 mm) (Ps-plastic, Eching, Germany). Subtracting inside items such as an axial fan, screws, supporting racks, and tubes, the chambers have a headspace volume of 0.33 m^3 and cover a surface area of 0.56 m^2. Depending on vegetation height, extension modules (interior dimensions: length 730, width 730, height 360 mm) can be connected to the chambers (total headspace volume is then 0.54 m^3) if needed over taller vegetation, but they were not used in this study. EPDM gaskets (20 mm × 15 mm) were attached to the bottom of each chamber in an aluminum u-channel to ensure gas-tight closure when chambers were operating. Up to three chambers can be combined into one system (Fig. 1b) with a joint control unit and autosampler or analyzer. Two custom-made temperature probes (Pt100) were installed inside and outside of each chamber to measure ambient air temperatures. Chambers were ventilated during measurements using an axial fan, which was mounted to produce a horizontally oriented airflow alongside the chamber walls to minimize interference with the natural steady-state soil efflux but to maximize proper mixing of the chamber headspace as was described in Drösler (2005). The air was sampled from the top center of the lids. Chamber operation was controlled by a logic module (Millenium 3, Crouzet, Hilden, Germany). An autosampler consisting of a membrane pump (operated at 0.8 L min^{-1}; NMP 830 KNDC, KNF Neuberger, Freiburg, Germany), an absorber to avoid water condensation within tubes (3.2 mm ID, 6.4 mm OD) (BEV-A-Line, ProLiquid GmbH, Überlingen, Germany), and valves, and an exchangeable rack for 162 headspace vials (20 mL, WICOM WIC 43200, Maienfeld, Germany) was connected to the chamber system. Chambers were lifted and moved down by a 24 V (DC) motor winch and were directed to the soil collar by the aluminum rack. After measurement events, the chamber was lifted to 1.18 m above ground and dragged backwards at a 45° angle to keep the soil and vegetation inside the soil collar under as natural conditions as possible (e.g., prevention of shading and undisturbed throughfall). To avoid pressure changes when setting the chamber on the collar, the chamber had a 1.5 m pressure compensation tube leading from the inside through the side wall of the chamber to the outside. Information about our chamber system including the construction plan is available to the scientific community and can be requested from the authors.

Table 1. Additional information on field campaigns.

	Braunschweig	Risø
Coordinates	52°17′52″ N, 10°26′36″ E	55°40′50″ N, 12°06′05″ E
Start observation period	13 Nov 2012	10 Apr 2013
End observation period	12 Dec 2012	24 Apr 2013
Total GC flux rates (n)	201	37
Total QCL flux rates (n)	187	158
Land use	Grassland	Willow field (harvested)
Fertilization, date	No fertilization	9 Apr 2013
Fertilization, amount	No fertilization	120 kg N ha^{-1}
Fertilization, type	No fertilization	Mineral (ammonium nitrate), N-P-K 21-3-10
Soil texture	Silty sand	Sandy loam
Soil type	Cambisol	Luvisol

2.2 Campaigns and measurement setup

Two field campaigns were conducted in fall 2012 in Braunschweig, Germany, and in spring 2013, at Risø Campus, Technical University of Denmark, using both GC and QCL chamber setups (see Table 1 for additional information). The chamber architecture was identical during the two campaigns. Sites and time periods were selected with the aim to compare chamber system performance under high- and low-flux conditions. Due to low temperatures and the lack of fertilizer application, we expected a low-exchange regime during the Braunschweig campaign, whereas higher fluxes were expected at Risø (higher temperatures and a substantial amount of fertilizer applied).

During parallel operation of GC and QCL, chambers were closed for 60 min at both sites to measure the concentration increase. When only QCL measurements were conducted, i.e., at Risø at DOY < 105.5 and > 108.5, chambers were closed for only 10 min. For the GC setup, four air samples were taken at 0, 20, 40, and 60 min after chamber closure to calculate one flux rate. Air samples (20 mL) were pumped through the tubing system using a membrane pump (3.2 L min^{-1}; NMP 830 KNDC, KNF Neuberger, Freiburg, Germany) and were injected into septum-capped vials. Two cannulas were automatically inserted through the septum, one cannula acting as sample air inlet until overpressure was established and the other cannula acting as outlet for cycling the air back to the chamber. Air samples were stored in the exchangeable rack of the autosampler unit and were analyzed in the GC lab of the Thünen Institute using a GC-2014 (Shi-

madzu, Duisburg, Germany; modified according to Loftfield et al., 1997) with an electron capture detector for N_2O analysis. Performance of the GC system was checked weekly by conducting 10 consecutive measurements of a standard gas with ambient N_2O concentration (320 ppb). Samples were only analyzed if the coefficient of variation of peak areas during this test was below 3 %.

Parallel to the autosampler setup for GC analysis, we operated our chamber system directly connected to a QCL (continuous-wave quantum cascade laser absorption spectrometer, model mini-QCLAS, Aerodyne Research Inc., Billerica, Massachusetts, USA; see Nelson et al. (2004) for principle of operation) in a thermo-controlled housing. Briefly, the laser is thermoelectrically cooled (Thermocube) to 25 °C, uses a 76 m path length, 0.5 L volume, and multiple-pass absorption cell for sampling, and operates at 40 Torr. It provides a measurement precision of 0.04 ppb (1σ) within an averaging interval of 1 s. Calibration is performed by continuously aligning the N_2O absorption peak of the sampled air to the standard of the HITRAN database (Rothman et al., 2009). A dry vacuum scroll pump (BOC Edwards XDS10, Sussex, UK) maintained a steady flow rate of 1.0 L min^{-1}. After passing the QCL cell, the sample air was cycled back to the respective chamber to avoid underpressure conditions and unintentional sucking of soil air into chambers. Data were stored on the QCL's internal hard drive at a frequency of 10 Hz.

The detection limit (LoD) of our QCL and GC setups could be estimated using our campaign data assuming stationary conditions during the low-flux campaign in Braunschweig. Taking the whole campaign into account, the calculated standard deviations were 2.5 and 7.5 µg m^{-2} h^{-1} for QCL and GC measurements, respectively. Thus, the resulting 2σ uncertainty range for QCL was 5.0 and for GC 15.0 µg m^{-2} h^{-1}. If only the first quarter of the Braunschweig campaign data are taken, i.e., a period where environmental conditions were less variable than over the whole campaign, the calculated standard deviations were 1.3 and 6.5 µg m^{-2} h^{-1} for QCL and GC measurements, respectively. Thus, the resulting 2σ uncertainty range for QCL was 2.6 and for GC 13.0 µg m^{-2} h^{-1}. These estimates can be regarded as an upper flux detection limit. A theoretical lower flux detection limit solely depends on the sensitivity of the analyzers. Precision of the QCL is 0.03 and 0.01 ppb when averaging over 1 and 60 s, respectively. Table 2 summarizes features of the chamber-analyzer system used in this study.

2.3 Flux calculation

GC-based N_2O fluxes using linear, robust linear (Huber, 1981), and modified Hutchinson–Mosier regression (HMR; cf. Pedersen et al., 2010) were calculated as described in Leiber-Sauheitl et al. (2014) after converting molar concentrations into mass concentrations using temperature but no pressure correction. Briefly, nonlinear flux estimation with the HMR method (R Core Team, 2012; HMR package version 0.3.1) was performed when four data points were available and all of the following criteria were met: (1) the HMR function could be fitted, (2) Akaike information criterion (AIC; Burnham and Anderson, 2004), which is a measure of (relative) model quality (i.e., gives fit quality penalized by the model's degrees of freedom) and can be used to compare the quality of different model fits to the same data set, was lower for HMR fit than for linear fit, (3) p value of flux calculated using HMR was lower than that from robust linear fit, and (4) the HMR flux was less than 4 times larger than the robust linear flux. Otherwise, robust linear regression or ordinary linear regression were used when four or three data points were available, respectively.

QCL-based fluxes were estimated using two different methods. We applied the nonlinear HMR model with a slightly modified parameterization (Eq. 1 this study; cf. Moffat, 2012) to the 60 min data set of a full chamber cycle (10 min cycle in Risø at DOY < 105.5 and > 108.5) and compared these fluxes with those resulting from an application of linear regression when only the first 3 min of data after chamber closure were used (cf. Sect. 3.2).

To investigate the frequently observed nonlinearity in chamber field data, we computed a quantitative parameter κ describing the curvature in N_2O concentration increase (or decrease) over time (60 and 10 min QCL data only). Based on the assumption of exponential gas concentration changes in the chamber (cf. Nakano et al., 2004) using

$$c(t) = c_{\max}\left(1 - \exp\left(\frac{-k}{c_{\max}}t\right)\right) + c_0, \quad (1)$$

with $c(t)$ being the N_2O concentration in the chamber at a certain point in time, $c_{\max}$ the maximum possible concentration range, c_0 the measured concentration at $t = 0$, and k the initial flux F_0 divided by the effective chamber height h, we estimated the N_2O soil–atmosphere flux as the first derivative of Eq. (1) evaluated at $t = 0$, i.e.,

$$c'(t)|_{t=0} = k, \quad (2)$$

and the curvature parameter κ as the second derivative of Eq. (1) evaluated at $t = 0$, i.e.,

$$c''(t)|_{t=0} = -\frac{k^2}{c_{\max}} = \kappa. \quad (3)$$

Units for concentrations $c(t)$, $c_{\max}$, and c_0 are grams per cubic meter, units for k are grams per cubic meter per second, and units for κ are grams per cubic meter per square second. Negative values of κ correspond to concave curvature indicating a plateauing, i.e., saturating concentration increase over time. Standard errors in this study were calculated as the parameter errors from the respective regression model with the algorithm being based on the Levenberg–Marquardt method (nlsLM function in R package "minpack.lm", R Core

Table 2. Features of the chamber-analyzer system used in this study.

	GC (model: Shimadzu GC-2014)	QCL (model: Aerodyne Research Inc. mini-QCLAS)
No. of chambers	3	3
Chamber closure time	60 min	60 min 10 min (recommended)
Sampling frequency	every 20 min	0.1 s (max) 5 s (recommended)
No. of concentration records per chamber run	4	36 000 in 60 min 6000 in 10 min
No. of chamber cycles per day	24 (max)	72 (recommended) 144 (max)
Maximum number of samples	168 (depending on autosampler size)	Limited only by data storage capacity of QCL's computer or external hard drive
Lag time	($\sim$ 10 s)	$\sim$ 10 s
N_2O flux detection limit ($\mu g\,N\,m^{-2}\,h^{-1}$)	13.0	2.6
Mean campaign N_2O flux ($\mu g\,N\,m^{-2}\,h^{-1}$)	BS (pref.[1]): 6.42 Risø (pref.[1]): 77.40	BS (lin.): 7.77 Risø (lin.[2]): 122.95
Mean campaign SE of N_2O fluxes ($\mu g\,N\,m^{-2}\,h^{-1}$)	BS (pref.[1]): 5.98 Risø (pref.[1]): 8.17	BS (lin.): 0.13 Risø (lin.[2]): 0.21
Median campaign N_2O flux ($\mu g\,N\,m^{-2}\,h^{-1}$)	BS (pref.[1]): 5.15 Risø (pref.[1]): 64.80	BS (lin.): 7.38 Risø (lin.[2]): 105.43
Median campaign SE of N_2O fluxes ($\mu g\,N\,m^{-2}\,h^{-1}$)	BS (pref.[1]): 5.04 Risø (pref.[1]): 4.72	BS (lin.): 0.10 Risø (lin.[2]): 0.17
Percentage of flux estimates where HMR could be fitted	BS: 8.5 % Risø: 37.9 %	BS: 100 % Risø: 100 %

GC – gas chromatograph; QCL – quantum cascade laser spectrometer; SE – standard error. [1] preferred means nonlinear HMR model was used if applicable, otherwise robust linear regression was taken. [2] Mean/median of DOY 105.5 to 108.5 to make values comparable to GC data set.

Team, 2012). Standard errors are solely associated with the flux calculation method and not with any kind of observational errors or issues related to measurement performance such as changes in flow rate, temperature sensitivity of the QCL, pump performance, or changes in chamber volume due to rough soil surfaces or plants in the chamber.

3 Results

3.1 Shape of concentration increase and curvature (κ) determination

Significantly different patterns in chamber N_2O concentration changes during the Braunschweig and Risø campaigns were observed (Fig. 2). While increases in the order of 10 to 20 ppb per hour (one chamber cycle) were found for the grassland site in Braunschweig, steep concentration increases measured on the harvested willow field at Risø were almost exclusively higher than 100 ppb per hour and reached maximum rates of over 650 ppb per hour in the period from DOY 105.5 to 108.5. For the low-exchange regime in Braunschweig, GC-based data points were highly scattered and rarely showed a clear increasing (or decreasing) tendency making flux calculations difficult. For the high-exchange regime at Risø, GC-based concentration data mostly showed well-defined increases and were similar to those obtained by the QCL system (cf. Sect. 3.3). The latter showed a precise and robust performance with clear base line levels and obvious chamber cycles during both campaigns. None of the QCL-based measurements revealed concentration decreases, i.e., negative fluxes (N_2O uptake), while chambers were closed.

Results of the investigation on quantifying the curvature in $c(t)$, expressed as κ, are given in Fig. 3. Extremely low absolute κ values between -10^{-4} and -10^{0} – indicating quasi linearity in $\partial c/\partial t$ – were almost exclusively found under low-flux conditions, whereas fluxes $> 100\,\mu g\,N\,m^{-2}\,h^{-1}$ were only observed when κ was $< -10^{1}$ (Fig. 3a).

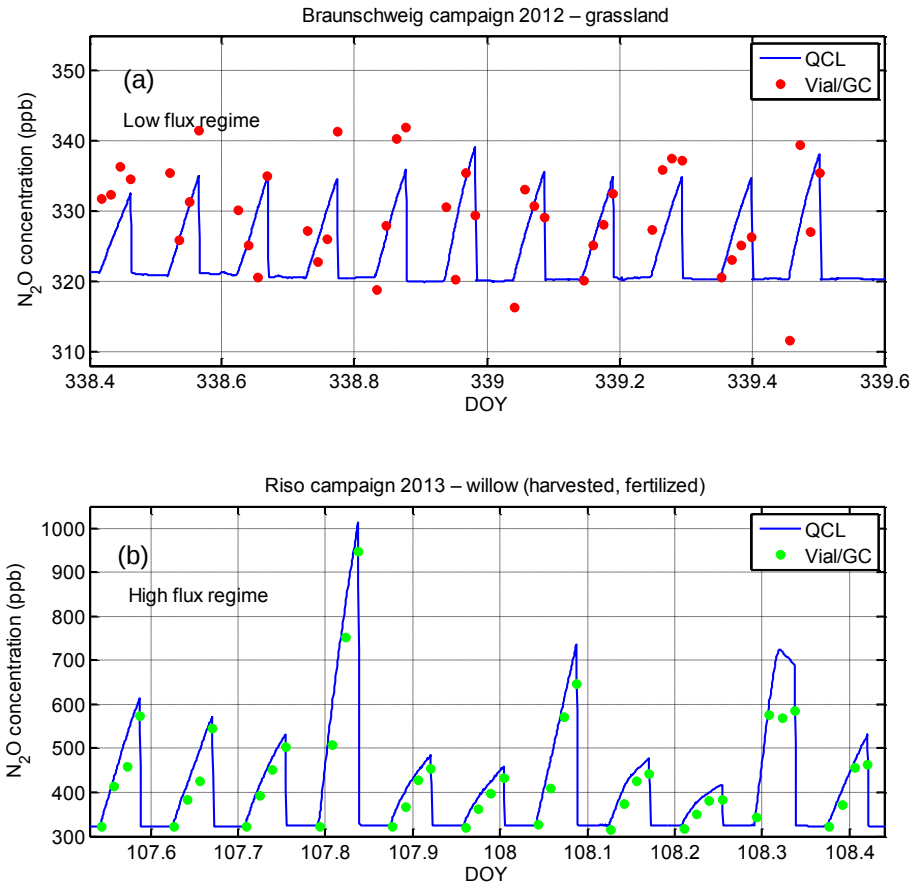

Figure 2. Examples of time series of N_2O chamber concentrations during the Braunschweig **(a)** and Risø campaign **(b)**. Chambers were periodically closed for 60 min. Vials were filled with sample air at t_0, t_{20}, t_{40}, and t_{60}. The QCL system was operated at a sampling frequency of 10 Hz; plotted are 1 min means.

3.2 Comparison of N_2O fluxes and their associated errors from linear and nonlinear regression models

With the QCL's high time resolution – in this study operated at the analyzer's maximum frequency of 10 Hz – we compared N_2O flux estimates based on 60 min (DOY 105.5 to 108.5) and 10 min (DOY < 105.5 and > 108.5) closure periods calculated by the modified HMR approach with those flux estimates that are based on the first 3 min of concentration data only and were calculated by linear regression. The Risø data set was used for this comparison because both high and low fluxes were observed. Flux estimates of the two approaches matched reasonably well; significant differences were only observed at very high rates (Fig. 4a, b). In total, 85 % of the variance in N_2O fluxes from 3 min closure could be explained by fluxes from 60 and 10 min closure (Fig. 4b). The relatively high slope of 1.80 was mainly caused by three exceptionally high fluxes where the 60 min method considerably overestimated values of the 3 min method. Standard errors of N_2O fluxes from both 3 and 60 min closure were extremely low, i.e., in the order of 0.2 % of the fluxes (Fig. 4c) with median values of 0.17 and 0.06 µg N m^{-2} h^{-1} and arithmetic means of 0.21 and 0.20 µg N m^{-2} h^{-1} for the 3 and 60 min closure flux estimates, respectively.

For better comparison with other studies, we also compared HMR-based fluxes with robust linearly calculated fluxes from our GC measurements when the full 60 min cycle was taken into account. A linear regression analysis (data not shown) resulted in a slope of 0.97 and an R^2 value of 0.86 under the high-flux regime in Risø with the data set of robust linearly calculated fluxes being the independent variable. The mean campaign flux value from HMR-based calculations was 22 % higher than the average campaign value of the robust linear method. The difference between the two methods was even higher under the low-flux regime in Braunschweig. Slope and R^2 value of a linear regression analysis were 1.82 and 0.42, respectively. Despite the high slope value, the mean campaign value of the robust linear method only reached 51 % of the value obtained from the HMR method.

A further intriguing analysis shows that standard errors were found to be invariant on QCL sampling frequency (Fig. 5). We simulated different sampling times ranging from

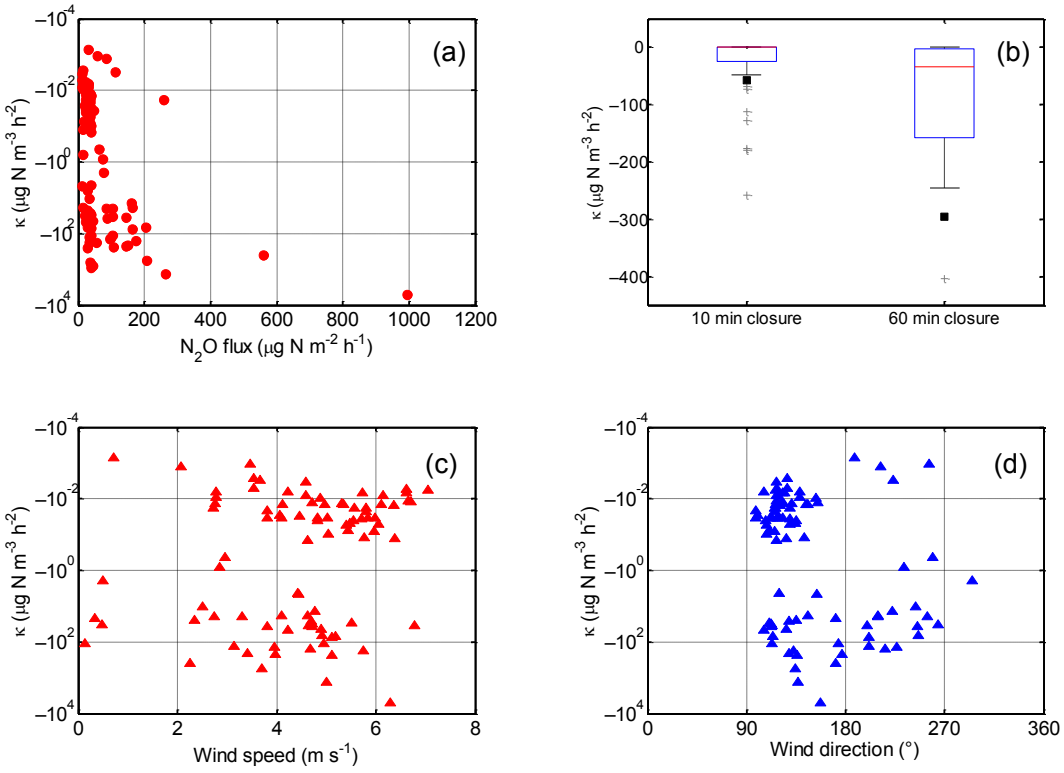

Figure 3. **(a)** Relationship between κ and N_2O fluxes calculated with an exponential model (see text for details). The parameter κ indicates the curvature, i.e., the second derivative of the exponential model used for flux calculation. Negative κ values correspond to concave functions, i.e., plateauing (saturating) N_2O concentration increases (cf. Fig. 2). **(b)** Box plot of κ values showing the difference between 10 and 60 min closure where black squares represent the arithmetic mean, red horizontal lines indicate the median, blue horizontal lines indicate lower and upper quartile values, black whiskers represent the interquartile range, and outliers from this range are plotted as grey crosses. To ensure better readability, the y axis is truncated at $-450\,\mu g\,N\,m^{-3}\,h^{-2}$. Thus, some outliers between -450 and $-10^4\,\mu g\,N\,m^{-3}\,h^{-2}$ are not shown. **(c, d)** Relationship between κ and wind speed **(c)** as well as κ and wind direction **(d)**. All data are taken from the quantum cascade laser system operated during the Risø campaign. Chambers were closed for 10 min at DOY < 105.5 and for 60 min at DOY > 105.5.

1/10 of a second to 25.6 s, which corresponds to a frequency of 0.0390625 Hz, by excluding the respective intervals from the original 10 Hz data set. Results show that the median of the standard error of the fluxes remains stable over a wide range of measurement frequencies. At a frequency class of 0.15 and lower (three boxes on the right-hand side of Fig. 5), which corresponds to a sampling time of ∼ 5 s and higher, lower and upper quartile values begin to deviate and the median changes slightly.

3.3 GC vs. QCL-based fluxes under low- and high-exchange regimes

Time series of N_2O fluxes and their associated standard errors using both the GC and the 3 min QCL linear regression method during the Braunschweig and Risø campaigns are given in Fig. 6. QCL fluxes in Braunschweig were at a constantly low level ranging between 2 and 16 µg $N\,m^{-2}\,h^{-1}$, whereas GC-based fluxes at the same site were scattered between −13 and 39 µg $N\,m^{-2}\,h^{-1}$. A linear regression revealed no significant relationship between GC and QCL fluxes with a very low coefficient of determination of 0.036 (Fig. 7a). While standard errors of the QCL method were always below 0.6 µg $N\,m^{-2}\,h^{-1}$, values of the GC method were distributed between 0.5 and 22.0 µg $N\,m^{-2}\,h^{-1}$. Although higher variability and higher standard errors in GC-based fluxes were evident, mean N_2O flux rates of the entire observation period were almost identical when comparing the two analyzer types. In total, 6.42 ± 5.98 and 7.77 ± 0.13 µg N $m^{-2}\,h^{-1}$ were found for the GC and the QCL method, respectively.

Under the high-exchange regime at Risø, N_2O fluxes of the two analyzer types matched considerably better (Fig. 6d). Although the willow field was already fertilized on DOY 99, N_2O fluxes did not start to increase until DOY 105 when a sharp rise in air temperature was observed. GC-based fluxes were lower than QCL-based fluxes (slope = 0.50) as in most cases a nonlinear model could not be fitted with only four data points. A linear regression between GC and QCL fluxes revealed a coefficient of determination of 0.48 (Fig. 7b). Standard errors of the QCL method were again ex-

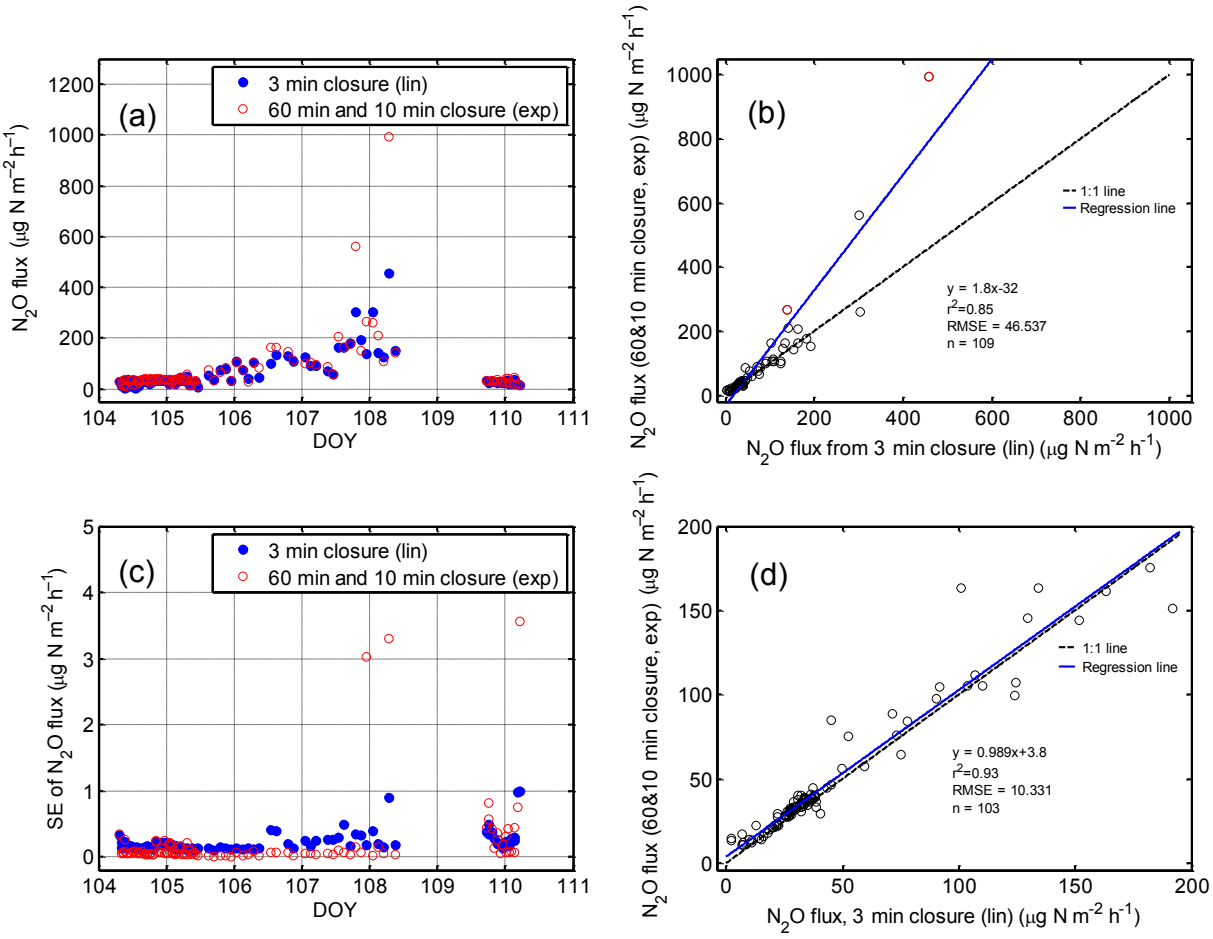

Figure 4. **(a)** Comparison of N_2O fluxes measured on a harvested willow field during the Risø campaign by the QCL system based on a linear model using only the first 3 min of data after chamber closure (filled blue circles) and an exponential model (open red circles) (see text) using either the full 60 min (DOY 105.5 to 108.5) or the full 10 min of data (DOY < 105.5 and > 108.5). **(b)** Linear regression analysis of N_2O fluxes from the exponential vs. the linear model. Red circles indicate fluxes where the underlying concentration data showed an unusual pattern with a steady linear start followed by a sudden relatively sharp bend with a lower linear increase afterwards (see Sect. 4.2 for details). **(c)** Standard errors of fluxes shown in **(a)**. **(d)** Same as **(b)**, but only for fluxes < 200 µg N m^{-2} h^{-1} with adapted regression.

tremely low, i.e., < 1 % of the flux value, and were always below 1.0 µg N m^{-2} h^{-1}, while those from the GC method were on average in the range of 5 to 10 % of the flux value. Parallel operation of both methods was conducted from DOY 105 to 108. During this period, the campaign means were 117.8 ± 0.2 and 77.4 ± 8.2 µg N m^{-2} h^{-1} for the QCL and GC method, respectively.

As standard errors of QCL-based N_2O fluxes were on a constantly low level, no dependency on flux value was observed in any of the campaigns (Fig. 7). The same was evident for GC-based fluxes in Braunschweig. At Risø, however, a slight but nonsignificant tendency of higher standard errors at higher flux rates was found. Only 8 % of GC data from Braunschweig met the criteria for flux calculation using the HMR model. At Risø, 38 % of GC data allowed for HMR flux calculation indicating that higher-exchange regimes favor the usage of an exponential model when using the GC method.

3.4 N_2O uptake and diurnal variation

Neither at Risø nor during the Braunschweig campaign was soil N_2O uptake observed when using QCL-based measurements. Only very few cases ($n = 5$) $c'(t)$ were initially found to be negative; however, these data, which exhibited abnormally high standard errors, were discarded due to mechanical malfunctioning of the chamber system as a result of non-closure caused by distorted guiding racks through very high wind speeds at Risø (cf. Sect. 3.3).

Regarding GC-based data in our study, 2 out of 37 fluxes in Risø were negative. Note that GC-based fluxes in Risø were only determined between DOY 105.5 and 108.5 when fluxes were elevated due to fertilizer application. In Braunschweig,

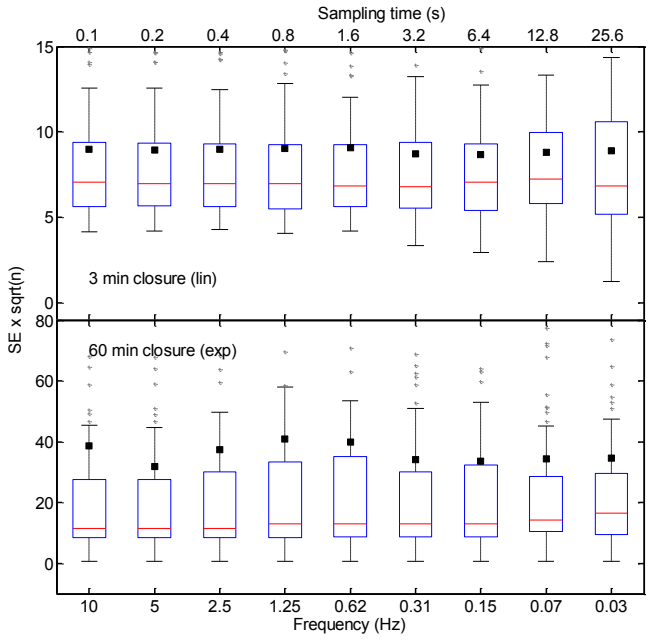

Figure 5. Box plots of standard errors of N_2O fluxes for different frequency classes and regression models used, i.e., linear regression with 3 min of data (upper panel) and the exponential HMR model with 60 min of data (lower panel). To avoid a pseudo-dependency on sample size, the standard errors (SEs) were normalized by multiplication with $\sqrt{n}$. Black squares represent the arithmetic mean, red horizontal lines indicate the median, blue horizontal lines indicate lower and upper quartile values, black whiskers represent the interquartile range, and outliers from this range are plotted as grey crosses.

however, nearly 25 %, i.e., 50 out of 201 flux rates, from the GC setup showed N_2O uptake with only 3 of the 50 negative flux rates being significant ($p < 0.05$; p values not corrected for multiple testing).

An investigation of the diurnal variability of N_2O fluxes showed that during the Braunschweig campaign – although only small differences were observed – the highest fluxes were found during midday and early afternoon ($\sim 8.7\,\mu g\,N\,m^{-2}\,h^{-1}$), while the lowest N_2O efflux was measured shortly before midnight and before sunrise (~ 7.2 and $7.3\,\mu g\,N\,m^{-2}\,h^{-1}$, respectively; Fig. 8), thereby following a commonly observed temperature-driven pattern (cf. Sect. 4.4). In Risø, however, we found the lowest fluxes of $\sim 18.2\,\mu g\,N\,m^{-2}\,h^{-1}$ at midday and the highest fluxes when it was dark, peaking before midnight at $\sim 32.0\,\mu g\,N\,m^{-2}\,h^{-1}$ (only data of DOY < 105.5 and > 108.5 were taken to exclude fertilizer effects). Error bars in Fig. 8 indicate the standard error of the mean from all flux values in each bin. Each bin contains fluxes from 3 h periods, i.e., from 00:00 to 03:00, 03:00 to 06:00, 06:00 to 09:00 CET, etc. The mean values in Fig. 8 are plotted in the center of each bin. Fluxes were binned due to irregular starting times of new chamber cycles. In general, a new chamber cycle could be started each full hour, but to get a more robust diurnal pattern, we decided to bin data in the abovementioned 3 h containers. While the diurnal variation of N_2O fluxes from the Risø campaign is significant ($p = 0.0059$), the diurnal variation found during the Braunschweig campaign is not, as the difference between mean minimum and maximum values is lower than the upper flux detection limit of $\sim 2.6\,\mu g\,N\,m^{-2}\,s^{-1}$.

4 Discussion

4.1 The curvature parameter κ as a chamber performance criterion

The high time resolution of QCL data allowed for a closer look at the shape of the concentration increase. The general form of the curve is determined by the rate of transport of a diffusing trace gas into the chamber headspace, which declines throughout deployment because any increase in the headspace concentration results in a corresponding decline in the vertical concentration gradient driving that transport (Rolston, 1986; Hutchinson et al., 2000; Livingston et al., 2006). The change in the rate of transport is the initial curvature kappa, i.e., the second derivative of the concentration change at $t = 0$.

The fact that extremely low negative κ values between -10^{-4} and -10^{0} – indicating quasi linearity in $\partial c/\partial t$ – were almost exclusively found under low-flux conditions, whereas fluxes $> 100\,\mu g\,N\,m^{-2}\,h^{-1}$ were only observed when κ was $< -10^{1}$ (Fig. 3a), means that at higher fluxes the curvature in $c(t)$ is concave, suggesting concentrations that tend to plateau over time with the saturation effect becoming larger at higher flux rates. Near-zero fluxes, however, corresponding to κ values around zero, indicate no considerable changes in N_2O concentrations and thus hardly any alteration of the vertical concentration gradient over time. Furthermore, closure time was found to have an impact on the magnitude of κ (Fig. 3b). Longer chamber deployment led to higher curvature in $c(t)$, which was expected as concentration gradients decline over time when a considerable flux is measured (cf. Hutchinson and Mosier, 1981; Livingston et al., 2006; Pedersen et al., 2010).

Our results imply that at low to moderately high flux rates $< 200\,\mu g\,N\,m^{-2}\,h^{-1}$ (cf. Fig. 4d) and/or short chamber closure, the slight nonlinearity in concentration change when calculating fluxes is of minor importance and the application of linear models is acceptable, particularly with regard to other commonly observed errors such as those originating from soil disturbance, chamber placement (Christiansen et al., 2011), temperature, and pressure and humidity perturbations (Parkin and Venterea, 2010). At higher fluxes, however, significant curvature in $c(t)$ expressed by large negative κ values will most likely lead to a substantial underestimation of fluxes when using linear regression instead of applying an exponential model for flux calculation (cf. Matthias et al.,

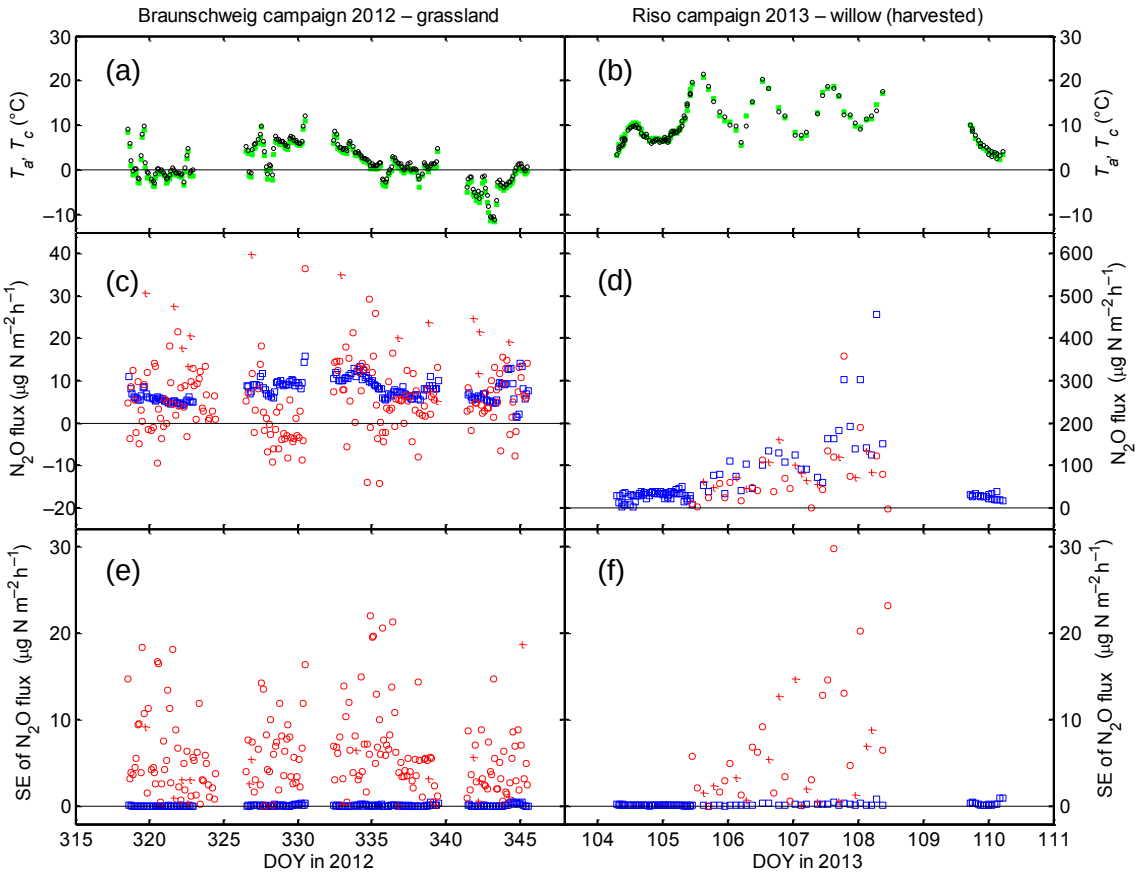

Figure 6. Time series of air (T_a, green markers) and chamber temperatures (T_c, black markers) **(a, b)**, N_2O fluxes and the respective standard errors of N_2O fluxes, during the Braunschweig **(c, e)** and the Risø campaign **(d, f)**. Blue markers indicate QCL data; red markers indicate GC data. Crosses are plotted for GC data when all criteria for flux calculation using the exponential HMR model were met (see text for details); otherwise circles are plotted indicating the usage of a linear model for flux calculation.

1978; Jury et al., 1982; Anthony et al., 1995; Kroon et al., 2008; Sect. 3.2). In principle, several other reasons making flux determination with linear or exponential models problematic may technically be found. These are exponentially increasing N_2O concentrations after chamber closure due to possible dispersion effects leading to biased analyzer readings when the elevated gas concentration is initially not uniformly mixed with the air inside the tubing, placement of the sample tube inlet at the top of the chamber lid leading to an establishment of a temporary concentration gradient in a weakly mixed chamber atmosphere, or an insufficient dimension of the pressure compensation tube leading to a push-back of air into the uppermost soil layer at the moment when the chamber is set onto the lid. However, none of these were observed during our campaigns, thereby indicating a robust setup and chamber design for reliable N_2O flux calculations.

We also investigated the possible effect of ambient wind speed and direction on concentration buildup characteristics (Fig. 3c and d, respectively) as differences between turbulence conditions outside the chamber may possibly vary from those conditions inside the chamber under changing wind speed. Theoretically, pores in the uppermost soil layer might be ventilated under high wind speed when no chamber is in place; thus, a close coupling of the flux to the atmosphere exists. Consequently, the establishment of a steady-state flux may be more postponed under these high wind speed conditions once the chamber is put onto the soil frame. Such time delay caused by a slow filling up of the previously ventilated pore space in parallel to the diffusion into the chamber might in principle explain exponentially increasing concentrations. However, κ values (Fig. 3c, d) and fluxes (not shown) were independent of both wind speed and direction, which is a further indicator that the chosen chamber design and setup can be used over a wide range of environmental conditions and neither seem to affect concentration buildup characteristics nor resulting flux magnitudes.

4.2 Closure time and measurement frequency – how long and how often is enough?

Reviewing past decades of field chamber measurements for studying the soil–atmosphere exchange of N_2O, several chal-

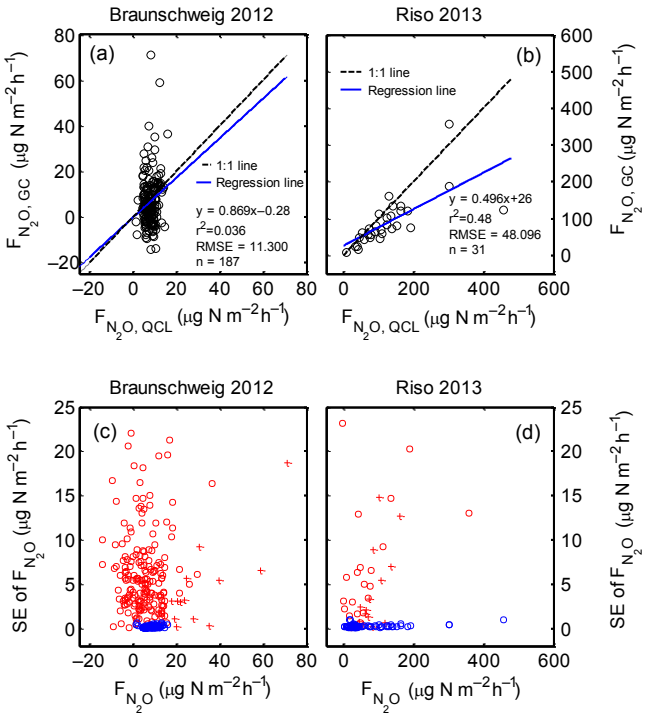

Figure 7. (a, b) GC vs. QCL-based N_2O fluxes. **(c, d)** Relationships between standard errors (SEs) of N_2O fluxes and the respective flux values. Blue markers indicate QCL data, which are all based on the 3 min linear calculation method. Red markers indicate GC data, which are based on the full 60 min data set. Crosses are plotted for GC data when all criteria for flux calculation using the exponential HMR model were met (see text for details); otherwise circles are plotted indicating the usage of a linear model for flux calculation.

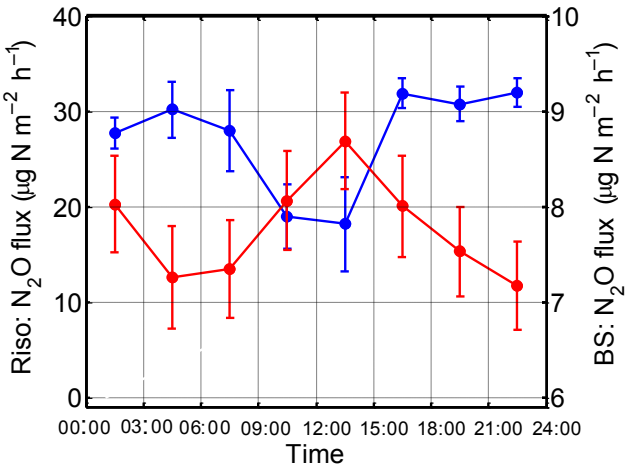

Figure 8. Mean diurnal courses of N_2O fluxes derived from QCL flux measurements during the Risø (blue line) and Braunschweig (red line) campaign. To exclude fertilization effects in Risø, only data from the low-flux period (DOY < 105.5 and > 108.5) were taken.

lenges and shortcomings emerged such as a limited number of replicates or the disturbance of the soil microenvironment due to chamber coverage and soil collar insertion (e.g., Hutchinson and Mosier, 1981; Parkin and Venterea, 2010). One way of getting a higher temporal resolution and thereby a higher number of replicates, and keeping soil disturbance as low as possible is to reduce the chamber closure period, which is also expected to decrease deviation from linearity in concentration increase.

The overestimation of the 60 min method compared to the 3 min method as shown in Fig. 4b, which causes a relatively high slope of 1.80, was mainly caused by three exceptionally high fluxes. In addition to any form of unintended interferences with the "natural steady-state flux" (for example, disturbances through macrofauna, fluctuating pump performance, or analyzer malfunctions due to internal recalibration during chamber deployment), much higher 60 min-based HMR fluxes compared to 3 min-based linear fluxes may be observed when one of the two following concentration increase patterns are observed.

1. A slow initial increase in concentrations followed by a steeper rise after some minutes. The slope of the linear fit will then be much lower than the one from the HMR fit (linear fit at t_0).

2. A steady linear start to the concentration increase followed by a sudden relatively sharp bend with a lower linear increase afterwards. The HMR fit will also have a much steeper slope at t_0 than the linear fit, which will be above the data points for the first few minutes.

Red dots in Fig. 4b indicate situations similar to those described under (2) above. Recent work, e.g., by Kroon et al. (2008) and Forbrich et al. (2010), demonstrated that emission estimates from closed-chamber measurements were significantly underestimated when using linear regression methods instead of the slope of an exponential function at the beginning of chamber closure. However, their linear regression models were applied to longer periods, i.e., to 10 min periods by Kroon et al. (2008) also using an Aerodyne QCL spectrometer and to 25 min periods by Forbrich et al. (2010) using a GC setup. Kroon et al. (2008) also showed that linear estimates differed by up to 60 % compared to those from exponential methods with a systematic error due to linear regression being in the same order as the estimated uncertainty due to temporal variation.

As shown in Fig. 4c, standard errors of N_2O fluxes from both 3 min and 60 min closure were extremely low, i.e., in the order of 0.2 % of the fluxes with median values of 0.17 and 0.06 µg $N\,m^{-2}\,h^{-1}$ and arithmetic means of 0.21 and 0.20 µg $N\,m^{-2}\,h^{-1}$ for the 3 and 60 min closure flux estimates, respectively. In comparison, Cowan et al. (2014a) also find low flux uncertainty of less than 1 to 2 µg $N\,m^{-2}\,h^{-1}$. This implies that limiting the chamber closure period to 3 min in beneficial in two ways. On the one hand, the soil column of interest is less disturbed by shorter coverage and/or

the number of replicates can be significantly increased. As these measurements are automated, no further manual work is required. On the other hand, standard errors of fluxes remain extremely low. However, it is recommended to extend the chamber closure period to a minimum of 5 and a maximum of 10 min as slightly delayed concentration increases under low-flux regimes may occur (in ~ 5 % of the cases in our study) and would lead to an underestimation of 3 min linear fluxes (see Fig. S1 in the Supplement). We therefore recommend skipping the first 2 min of data to guarantee undisturbed conditions that might have been caused at the moment when the chamber is set on the soil collar. The "dead time" of the system, i.e., the time that passes between the moment when an air sample leaves the chamber and the moment when it reaches the analyzer, was ~ 10 s – given a tube length of 10 m, a flow rate of $1\,\mathrm{L\,min^{-1}}$, and an ID of the tube of 4.6 mm – and was already considered in the recommendation.

Standard errors of N_2O fluxes were found to be invariant on QCL sampling frequency (Fig. 5). The conclusion we can draw from this finding is that chamber operators – in the case of an analyzer with a precision like the QCL presented in this study being available – can reduce their sampling time down to 5 s without risking an increase in the standard error of the flux, which would still be on a much lower level than those obtained from GC measurements (cf. results in Sect. 3.2).

4.3 Differences between GC and QCL-based fluxes

Our comparison of GC vs. QCL fluxes revealed that despite much higher precision, robustness, and temporal resolution in QCL measurements, GC is still a useful method to determine the average campaign N_2O soil efflux. Although single flux values particularly under low-exchange regimes did not match well, campaign means and medians were similar to those obtained by the QCL method. Under high-exchange regimes, however, flux patterns matched considerably better but resulted in larger absolute errors when comparing the campaign average, thereby leading to systematic errors (in our case an underestimation) when using the GC method at high N_2O fluxes for the assessment of N balances. However, given the fact that the bulk of the annual efflux occurs after management events on a relatively short timescale (Flechard et al., 2007; Skiba et al., 2013), usage of a GC-based system will be prone to large uncertainties (cf. Fig. 7).

While only 8 % of GC data from the Braunschweig campaign met the criteria for flux calculation using the HMR model, 38 % of GC from the Risø data allowed for HMR flux calculation, indicating that higher-exchange regimes favor the usage of an exponential model when using the GC method. Similar findings (37 % allowance for nonlinear model application) were reported by Petersen et al. (2011). Forbrich et al. (2010) found percentages of 13.6, 19.2, and 9.8 % of GC measurements on hummocks, lawns, and flarks, respectively, which were best fitted with an exponential model. Their measurements, however, were made for methane fluxes and under an even larger $\partial c/\partial t$ range than was prevalent in our two campaigns. The fact that higher fluxes in our study were associated with lower standard errors and accepted HMR application corresponds well with κ findings in Sect. 3.1 indicating that higher curvature in $c(t)$ coincided with higher fluxes (Fig. 3b).

In general, chamber architecture is essential for headspace concentration buildup patterns given certain enclosure times, activity levels and headspace mixing. Our new chamber system performed well during the two campaigns for both analyzer setups. Through its specific design with not only vertically but also horizontally moving chambers, it will keep the soil column under relatively natural conditions. The only problem emerged at Risø when the guiding racks were slightly distorted under high wind speed conditions, i.e., when half-hourly means of wind speed were higher than $6\,\mathrm{m\,s^{-1}}$. However, this problem could easily be fixed by tightening the guy wires that are attached to the aluminum rack. Commonly observed winter problems such as unnatural accumulation of snow inside the chamber and rime ice formation on the guiding racks and soil frame were not tested within this study but will likely affect the ease of operation during harsh winter conditions.

4.4 Enabling investigations of flux pattern characteristics

From an ecological point of view, QCL measurements offer a new opportunity for robust quantification of soil N_2O consumption. As N_2O uptake via denitrification exists in theory and could be shown under controlled lab conditions (e.g., Firestone and Davidson, 1989), it has been a major challenge to measure reliable fluxes in the field due to the fact that the magnitude of N_2O uptake by soils is usually very low (Schlesinger, 2013) and thereby problematic to be determined by GC measurements that are subjected to low signal-to-noise ratios (e.g., Brümmer et al., 2008).

Our QCL-based measurements under the given soil, temperature, and moisture conditions at Risø and Braunschweig did not result in any soil N_2O uptake fluxes. In the study by Cowan et al. (2014b), approx. 10 % of their fluxes on grazed grassland and barley sites were negative. However, only 4 out of 115 negative fluxes were above the LoD of the method, which was estimated to be $4\,\mu\mathrm{g\,N\,m^{-2}\,h^{-1}}$, thus being similar to ours (cf. Table 2).

GC-based data in our study showed 2 out of 37 and 50 out of 201 negative fluxes in Risø and Braunschweig, respectively. In Risø, only 3 of the 50 negative flux rates were found to be significant ($p < 0.05$; p values not corrected for multiple testing), thus stressing the challenge of a robust determination of soil consumption of this important greenhouse gas when using the common vial–GC approach. Due to the fact that in this study no N_2O soil uptake was found when using the much more reliable QCL setup, a further investigation of

this topic on a variety of soil types under different land uses, plant communities, and climatic conditions is highly desired.

Besides investigating possible N_2O soil uptake, the QCL methodology offers the opportunity to study diurnal variability of N_2O fluxes. In a recent study by Shurpali et al. (2016), it has been pointed out that neglecting diurnal variations leads to uncertainties in terrestrial N_2O emission estimates, and they should therefore be taken into account carefully when calculating nitrogen budgets. Similar to our study (Fig. 8), Shurpali et al. (2016) found reversed diurnal patterns under differing flux magnitudes. Intriguingly, when mean N_2O fluxes were in a range between 12 and 35 µg $N\,m^{-2}\,h^{-1}$, in both this study (Risø low-flux regime) and Shurpali et al. (2016), the highest fluxes were found during nighttime and the lowest fluxes around midday. A contrasting diurnal pattern was observed when fluxes were lower than during the Risø campaign, i.e., in Braunschweig (7.2 to 8.7 µg $N\,m^{-2}\,h^{-1}$), or much higher due to fertilizer application as in Shurpali et al. (2016) (230 to 475 µg $N\,m^{-2}\,h^{-1}$). In the latter campaigns, mean N_2O fluxes were highest at midday and lowest during the nighttime, which corresponds to earlier findings (e.g., Christensen, 1983; Du et al., 2006; Parkin and Kaspar, 2006; Brümmer et al., 2008; Alves et al., 2012) where temperature was proved to be the main controlling factor for N_2O soil–atmosphere exchange. Our study highlights that through their high time resolution, QCL-based measurements will not only help enhance process understanding of N_2O exchange by disentangling the strength of different drivers of N_2O production like temperature, soil moisture, nitrogen availability, and microbial activity, but they also have the potential to provide new insight into bidirectional exchange characteristics of other trace gases such as CH_4, which can be sampled simultaneously with our chamber system depending on the analyzer type used.

5 Conclusions

A new chamber system for automated measurements of soil–atmosphere trace gas exchange was developed. The system was tested for N_2O flux detection in a conventional vial air sampling setup and with a directly connected QCL spectrometer under low- and high-exchange regimes. Through its specific design, the system prevents measurement spots from unintended shading and minimizes disturbance of throughfall, thereby complying with high quality requirements of long-term observation studies and research infrastructures. Curvature in $\partial c/\partial t$ proved to be invariant with wind speed and direction. High correlation (slope = 0.99; $R^2 = 0.93$) was found when comparing linear vs. modified HMR flux calculation methods for $F_{N_2O} < 200$ µg $N\,m^{-2}\,h^{-1}$. Intriguingly, mean campaign N_2O fluxes measured by GC and QCL of 6.42 and 7.77 µg $N\,m^{-2}\,h^{-1}$, respectively, matched fairly well under low-flux conditions, whereas under high-flux conditions a significant deviation was observed (77.40 vs. 122.95 µg $N\,m^{-2}\,h^{-1}$ from GC and QCL, respectively). While mean standard errors were in a range of 10 to 93 % of the N_2O flux in low- to high-exchange regimes when using the GC approach, extremely low values for standard errors of 0.2 to 1.7 % of the flux under different exchange conditions were found for QCL measurements. When a fast-response analyzer is available, we recommend reducing chamber closure time to a maximum of 10 min and applying linear regression to a 3 min data window by rejecting the first 2 min after closure and a measurement frequency of 0.2 Hz, i.e., a sampling output of every 5 s. Furthermore, with its high precision and temporal resolution, QCL technology provides a powerful tool to investigate highly debated topics such as diurnal flux variability and soil N_2O uptake.

Data availability. Data are available and can be requested from the corresponding author (christian.bruemmer@thuenen.de).

The Supplement related to this article is available online at doi:10.5194/bg-14-1365-2017-supplement.

Competing interests. The authors declare that they have no conflict of interest.

Acknowledgements. This study was supported by the Thünen Institute of Climate-Smart Agriculture through the German Federal Ministry of Food and Agriculture (BMEL) as well as the Integrated Carbon Observation System (ICOS) infrastructure through the Federal Ministry of Research and Education (BMBF). Funding for Christian Brümmer and Jeremy J. Rüffer by the BMBF Junior Research Group NITROSPHERE under support code FKZ 01LN1308A is greatly acknowledged. We highly appreciate logistical support during the Risø measurements, which were conducted in the framework of the InGOS project. The excellent introduction and valuable help on laser spectrometer operation and maintenance by David D. Nelson and Mark Zahniser is gratefully acknowledged. Many thanks are owed to Florian Hackelsperger from the experimental research station of the Institute of Animal Nutrition for technical support during the Braunschweig campaign as well as Kerstin Gilke and Andrea Oehns-Rittgerodt for N_2O analyses in the GC lab. Michel Bechtold is thanked for discussing and calculating dispersion estimates.

Edited by: X. Wang
Reviewed by: two anonymous referees

References

Alves, B. J. R., Smith, K. A., Flores, R. A., Cardoso, A. S., Oliveira, W. R. D., Jantalia, C. P., Urquiaga, S., and Boddey, R. M.: Selection of the most suitable sampling time for static chambers for the estimation of daily mean N_2O flux from soils, Soil Biol. Biochem., 46, 129–135, 2012.

Ammann, C., Wolff, V., Marx, O., Brümmer, C., and Neftel, A.: Measuring the biosphere-atmosphere exchange of total reactive nitrogen by eddy covariance, Biogeosciences, 9, 4247–4261, doi:10.5194/bg-9-4247-2012, 2012.

Anthony, W. H., Hutchinson, G. L., and Livingston, G. P.: Chamber measurement of soil–atmosphere gas exchange: Linear vs. diffusion-based flux models, Soil Sci. Soc. Am. J., 59, 1308–1310, 1995.

Baldocchi, D. D., Falge, E., Gu, L., Olson, R., Hollinger, D., Running, S., Anthoni, P., Bernhofer, C., Davis, K., Evans, R., Fuentes, J., Goldstein, A., Katul, G., Law, B.E., Lee, X., Malhi, Y., Meyers, T., Munger, W., Oechel, W., Paw U, K. T., Pilegaard, K., Schmid, H. P., Valentini, R., Verma, S., Vesala, T., Wilson, K., and Wofsy, S. C.: FLUXNET: A new tool to study the temporal and spatial variability of ecosystem-scale carbon dioxide, water vapor and energy flux densities, B. Am. Meteorol. Soc., 82, 2415–2434, 2001.

Brümmer, C., Brüggemann, N., Butterbach-Bahl, K., Falk, U., Szarzynski, J., Vielhauer, K., Wassmann, R., and Papen, H.: Soil-atmosphere exchange of N_2O and NO in near-natural savanna and agricultural land in Burkina Faso (W. Africa), Ecosystems, 11, 582–600, 2008.

Brümmer, C., Black, T. A., Jassal, R. S., Grant, N. J., Spittlehouse, D. L., Chen, B., Nesic, Z., Amiro, B. D., Arain, M. A., Barr, A. G., Bourque, C. P. A., Coursolle, C., Dunn, A. L., Flanagan, L. B., Humphreys, E. R., Lafleur, P. M., Margolis, H. A., McCaughey, J. H., and Wofsy, S. C.: How climate and vegetation type influence evapotranspiration and water use efficiency in Canadian forest, peatland and grassland ecosystems, Agr. Forest Meteorol., 153, 14–30, 2012.

Brümmer, C., Marx, O., Kutsch, W. L., Ammann, C., Wolff, V., Fléchard, C. R., and Freibauer, A.: Fluxes of total reactive atmospheric nitrogen ($\sum N_r$) using eddy covariance above arable land, Tellus B, 65, 19770, doi:10.3402/tellusb.v65i0.19770, 2013.

Burnham, K. P. and Anderson, D. R.: Multimodel Inference: Understanding AIC and BIC in Model Selection, Sociol. Method. Res., 33, 261–304, 2004.

Butterbach-Bahl, K., Baggs, E. M., Dannenmann, M., Kiese, R., and Zechmeister-Boltenstern, S.: Nitrous oxide emissions from soils: how well do we understand the processes and their controls?, Philos. T. Roy. Soc. B, 368, 20130122, doi:10.1098/rstb.2013.0122, 2013.

Castaldi, S., de Grandcourt, A., Rasile, A., Skiba, U., and Valentini, R.: CO_2, CH_4 and N_2O fluxes from soil of a burned grassland in Central Africa, Biogeosciences, 7, 3459–3471, doi:10.5194/bg-7-3459-2010, 2010.

Chapuis-Lardy, L., Wrage, N., Metay, A., Chotte, J. L., and Bernoux, M.: Soils, a sink for N_2O? A review, Glob. Change Biol., 13, 1–17, 2007.

Christiansen, J. R., Korhonen, J. F. J., Juszczak, R., Giebels, M., and Pihlatie, M.: Assessing the effects of chamber placement, manual sampling and headspace mixing on CH_4 fluxes in a laboratory experiment, Plant Soil, 343, 171–185, 2011.

Christensen, S.: Nitrous oxide emission from a soil under permanent grass: Seasonal and diurnal fluctuations as influenced by manuring and fertilization, Soil Biol. Biochem. ,15, 531–536, 1983.

Cowan, N. J., Famulari, D., Levy, P. E., Anderson, M., Bell, M. J., Rees, R. M., Reay, D. S., and Skiba, U. M.: An improved method for measuring soil N_2O fluxes using a quantum cascade laser with a dynamic chamber, Eur. J. Soil Sci., 65, 643–652, doi:10.1111/ejss.12168, 2014a.

Cowan, N. J., Famulari, D., Levy, P. E., Anderson, M., Reay, D. S. and Skiba, U. M.: Investigating uptake of N_2O in agricultural soils using a high-precision dynamic chamber method, Atmos. Meas. Tech., 7, 4455–4462, doi:10.5194/amt-7-4455-2014, 2014b.

Dannenmann, M., Gasche, R., Ledebuhr, A., Holst, T., Mayer, H., and Papen, H.: The effect of forest management on trace gas exchange at the pedosphere-atmosphere interface in beech (Fagus sylvatica L.) forests stocking on calcareous soils, Eur. J. Forest Res., 126, 331–346, 2007.

Denmead, O. T., MacDonald, B. C. T., Bryant, G., Naylor, T., Wilson, S., Griffith, D. W. T., Wang, W. J., Salter, B., White, I., and Moody, P. W.: Emissions of methane and nitrous oxide from Australian sugarcane soils, Agr. Forest Meteorol., 150, 748–756, 2010.

Donoso, L., Santana, R., and Sanhueza, E.: Seasonal variation in N_2O fluxes at a tropical savanna site: soil consumption of N_2O during the dry season, Geophys. Res. Lett., 20, 1379–1382, 1993.

Drösler, M.: Trace gas exchange and climatic relevance of bog ecosystems, Southern Germany, Doctoral thesis, TU München, 1–182, 2005.

Du, R., Lu, D., and Wang, G.: Diurnal, seasonal, and inter-annual variations of N_2O fluxes from native semi-arid grassland soils of Inner Mongolia, Soil Biol. Biochem., 38, 3474–3482, 2006.

Firestone, M. K. and Davidson, E. A.: Microbiological basis of NO and N_2O production and consumption in soil, in: Exchange of trace gases between terrestrial ecosystems and the atmosphere, edited by: Andreae, M. O. and Schimel, D. S., Chichester: John Wiley and Sons Ltd., 7–21, 1989.

Flechard, C. R., Ambus, P., Skiba, U., Rees, R. M., Hensen, A., van Amstel, A., van den Pol-van Dasselaar, A., Soussana, J.-F., Jones, M., Clifton-Brown, J., Raschi, A., Horvath, L., Neftel, A., Jocher, M., Ammann, C., Leifeld, J., Fuhrer, J., Calanca, P., Thalman, E., Pilegaard, K., Di Marco, C., Campbell, C., Nemitz, E., Hargreaves, K. J., Levy, P. E., Ball, B. C., Jones, S. K., van de Bulk, W. C. M., Groot, T., Blom, M., Domingues, R., Kasper, G., Allard, V., Ceschia, E., Cellier, P., Laville, P., Henault, C., Bizouard, F., Abdalla, M., Williams, M., Baronti, S., Berretti, F., and Grosz, B.: Effects of climate and management intensity on nitrous oxide emissions in grassland systems across Europe, Agr. Ecosyst. Environ., 121, 135–152, 2007.

Flessa, H. Ruser, R., Schilling, R., Loftfield, N., Munch, J. C., Kaiser, E. A., and Beese, F.: N_2O and CH_4 fluxes in potato fields: automated measurement, management effects and temporal variation, Geoderma, 105, 307–325, 2002.

Forbrich, I., Kutzbach, L., Hormann, A., and Wilmking, M.: A comparison of linear and exponential regression for estimating diffusive CH_4 fluxes by closed-chambers in peatlands, Soil Biol. Biochem., 42, 507–515, 2010.

Hensen, A., Groot, T. T., van den Bulk, W. C. M., Vermeulen, A. T., Olesen, J. E., and Schelde, K.: Dairy farm CH_4 and N_2O emissions, from one square metre to the full farm scale, Agr. Ecosyst. Environ., 112, 146–152, 2006.

Horii, C. V., Munger, J. W., and Wofsy, S. C.: Fluxes of nitrogen oxides over a temperate deciduous forest, J. Geophys. Res., 109, D08305, doi:10.1029/2003JD004326, 2004.

Huber, P. J.: Robust Statistics, J. Wiley, New York, 1981.

Hutchinson, G. L. and Mosier, A. R.: Improved soil cover method for field measurement of nitrous oxide fluxes, Soil Sci. Soc. Am. J., 45, 311–316, 1981.

Hutchinson, G. L., Livingston, G. P., Healy, R. W., and Striegl, R. G.: Chamber measurement of surface–atmosphere trace gas exchange: Dependence on soil, interfacial layer, and source/sink properties, J. Geophys. Res., 105, 8865–8875, 2000.

IPCC: Climate Change 2013: The Physical Science Basis. Contribution of Working Group I to the Fifth Assessment Report of the Intergovernmental Panel on Climate Change, edited by: Stocker, T. F., Qin, D., Plattner, G.-K., Tignor, M., Allen, S. K., Boschung, J., Nauels, A., Xia, Y., Bex, V., and Midgley, P. M., Cambridge University Press, CambridgeUnited Kingdom and New York, NY, USA, 2013.

Jassal, R. S., Black, T. A., Chen, B., Roy, R., Nesic, Z., Spittlehouse, D. L., and Trofymow, J. A.: N_2O emissions and carbon sequestration in a nitrogen-fertilized Douglas fir stand, J. Geophys. Res., 113, G04013, doi:10.1029/2008JG000764, 2008.

Jassal, R. S., Black, T. A., Roy, R., and Ethier, G.: Effect of nitrogen fertilization on CH_4 and N_2O fluxes, and bole and soil respiration, Geoderma, 162, 182–186, 2011.

Jones, S. K., Famulari, D., Di Marco, C. F., Nemitz, E., Skiba, U. M., Rees, R. M., and Sutton, M. A.: Nitrous oxide emissions from managed grassland: a comparison of eddy covariance and static chamber measurements, Atmos. Meas. Tech., 4, 2179–2194, doi:10.5194/amt-4-2179-2011, 2011.

Jury, W. A., Letey, J., and Collins, T.: Analysis of chamber methods used for measuring nitrous oxide production in the field, Soil Sci. Soc. Am. J., 46, 250–256, 1982.

Kroon, P. S., Hensen, A., van den Bulk, W. C. M., Jongejan, P. A. C., and Vermeulen, A. T.: The importance of reducing the systematic error due to non-linearity in N_2O flux measurements by static chambers, Nutr. Cycl. Agroecosys., 82, 175–186, 2008.

Kroon, P. S., Schuitmaker, A., Jonker, H. J. J., Tummers, M. J., Hensen, A., and Bosveld, F. C.: An evaluation by laser Doppler anemometry of the correction algorithm based on Kaimal cospectra for high frequency losses of EC flux measurements of CH_4 and N_2O, Agr. Forest Meteorol., 150, 794–805, 2010.

Kutsch, W. L., Aubinet, M., Buchmann, N., Smith, P., Osborne, B., Eugster, W., Wattenbach, M., Schrumpf, M., Schulze, E. D., Tomelleri, E., Ceschia, E., Bernhofer, C., Beziat, P., Carrara, A., Di Tommasi, P., Grünwald, T., Jones, M., Magliulo, V., Marloie, O., Moureaux, C., Olioso, A., Sanz, M. J., Saunders, M., Sogaard, H., and Ziegler, W.: The net biome production of full crop rotations in Europe, Agr. Ecosyst. Environ., 139, 336–345, 2010.

Kutzbach, L., Schneider, J., Sachs, T., Giebels, M., Nykänen, H., Shurpali, N. J., Martikainen, P. J., Alm, J., and Wilmking, M.: CO_2 flux determination by closed-chamber methods can be seriously biased by inappropriate application of linear regression, Biogeosciences, 4, 1005–1025, doi:10.5194/bg-4-1005-2007, 2007.

Laville, P., Lehuger, S., Loubet, B., Chaumartin, F., and Cellier, P.: Effect of management, climate and soil conditions on N_2O and NO emissions from an arable crop rotation using high temporal resolution measurements, Agr. Forest Meteorol., 151, 228–240, 2011.

Leiber-Sauheitl, K., Fuß, R., Voigt, C., and Freibauer, A.: High CO_2 fluxes from grassland on histic Gleysol along soil carbon and drainage gradients, Biogeosciences, 11, 749–761, doi:10.5194/bg-11-749-2014, 2014.

Livesley, S.J., Grover, S., Hutley, L.B., Jamali, H., Butterbach-Bahl, K., Fest, B., Beringer, J., and Arndt, S.: Seasonal variation and fire effects on CH_4, N_2O and CO_2 exchange in savanna soils of northern Australia, Agr. Forest Meteorol., 151, 1440–1452, 2011.

Livingston, G. P., Hutchinson, G. L., and Spartalian, K.: Trace gas emission in chambers: a non-steady-state diffusion model, Soil Sci. Soc. Am. J., 70, 1459–1469, 2006.

Loftfield, N., Flessa, H., Augustin, J., and Beese, F.: Automated gas chromatographic system for rapid analysis of the trace gases methane, carbon dioxide, and nitrous oxide, J. Environ. Qual., 26, 560–564, 1997.

Lohila, A., Aurela, M., Hatakka, J., Pihlatie, M., Minkkinen, K., Penttil, T., and Laurila, T.: Responses of N_2O fluxes to temperature, water table and N deposition in a northern borealfen, Eur. J. Soil Sci., 61, 651–661, 2010.

Matthias, A. D., Yarger, D. N., and Weinbeck, R. S.: A numerical evaluation of chamber methods for determining gas fluxes, Geophys. Res. Lett., 5, 765–768, 1978.

Merbold, L., Eugster, W., Stieger, J., Zahniser, M., Nelson, D. D., and Buchmann, N.: Greenhouse gas budget (CO_2, CH_4 and N_2O) of intensively managed grassland following restoration, Glob. Change Biol., 20, 1913–1928, 2014.

Moffat, A. M.: A new methodology to interpret high resolution measurements of net carbon fluxes between terrestrial ecosystems and the atmosphere, Doctoral Thesis, Department of Mathematics and Computer Science, Friedrich Schiller University, Jena, 2012.

Nakano, T., Sawamoto, T., Morishita, T., Inoue, G., and Hatano, R.: A comparison of regression methods for estimating soil–atmosphere diffusion gas fluxes by a closed-chamber technique, Soil Biol. Biochem. 36, 107–113, 2004.

Neftel, A., Ammann, C., Fischer, C., Spirig, C., Conen, F., Emmenegger, L., Tuzson, B., and Wahlen, S.: N_2O exchange over managed grassland: Application of a quantum cascade laser spectrometer for micrometeorological flux measurements, Agr. Forest Meteorol., 150, 775–785, 2010.

Nelson, D. D., McManus, B., Urbanski, S., Herndon, S., and Zahniser, M. S.: High precision measurements of atmospheric nitrous oxide and methane using thermoelectrically cooled mid-infrared quantum cascade lasers and detectors, Spectrochim. Acta A, 60, 3325–3335, 2004.

Papen, H. and Butterbach-Bahl, K.: A 3-year continuous record of nitrogen trace gas fluxes from untreated and limed soil of a N-saturated spruce and beech forest ecosystem in Germany, 1. N_2O emissions, J. Geophys. Res., 104, 18487–18503, 1999.

Parkin, T. B. and Kaspar, T. C.: Nitrous Oxide Emissions from Corn–Soybean Systems in the Midwest, J. Environ. Qual., 35, 1496–1506, 2006.

Parkin, T. B. and Venterea, R. T.: Chamber-based trace gas flux measurements, USDA-ARS GRACEnet Project Protocols, Chapter 3, 2010.

Pedersen, A. R., Petersen, S. O., and Schelde, K.: A comprehensive approach to soil-atmosphere trace-gas flux estimation with static chambers, Eur. J. Soil Sci., 61, 888–902, 2010.

Petersen, S. O., Mutegi, J. K., Hansen, E. M., and Munkholm, L. J.: Tillage effects on N_2O emissions as influenced by a winter cover crop, Soil Biol. Biochem., 43, 1509–1517, 2011.

Pihlatie, M. K., Christiansen, J. R., Aaltonen, H., Korhonen, J. F., Nordbo, A., Rasilo, T., Benanti, G., Giebels, M., Helmy, M., Sheehy, J., Jones, S., Juszczak, R., Klefoth, R., Lobo-do-Vale, R., Rosa, A. P., Schreiber, P., Serca, D., Vicca, S., Wolf, B., and Pumpanen, J.: Comparison of static chambers to measure CH_4 emissions from soils, Agr. Forest. Meteorol., 171, 124–136, 2013.

R Core Team: R: A language and environment for statistical computing, available at: http://www.R-project.org/ (last access: 13 March 2017), 2012.

Rinne, J., Pihlatie, M., Lohila, A., Thum, T., Aurela, M., Tuovinen, J., Laurila, T., and Vesala, T.: Nitrous oxide emissions from a municipal landfill, Environ. Sci. Technol., 39, 7790–7793, 2005.

Rolston, D. E.: Gas diffusivity, in: Methods of soil analysis, Part 1. Physical and mineralogical methods, edited by: Klute, A., 2nd Edn., ASA and SSSA, Madison, WI, Agron. Monogr., 9, 1089–1102, 1986.

Rosenkranz, P., Brüggemann, N., Papen, H., Xu, Z., Horváth, L., and Butterbach-Bahl, K.: Soil N and C trace gas fluxes and microbial soil N turnover in a sessile oak (Quercus petraea (Matt.) Liebl.) forest in Hungary, Plant Soil, 286, 301–22, 2006.

Rothman, L. S., Gordon, I. E., Barbe, A., Benner, D. C., Bernath, P. F., Birk, M., Boudon, V., Brown, L. R., Campargue, A., Champion, J.-P., Chance, K., Coudert, L. H., Dana, V., Devi, V. M., Fally, S., Flaud, J.-M., Gamache, R. R., Goldman, A., Jacquemart, D., Kleiner, I., Lacome, N., Lafferty, W., Mandin, J.-Y., Massie, S. T., Mikhailenko, S. N., Miller, C. E., Moazzen-Ahmadi, N., Naumenko, O. V., Nikitin, A. V., Orphal, J., Perevalov, V. I., Perrin, A., Predoi-Cross, A., Rinsland, C. P., Rotger, M., Simeckova, M., Smith, M. A. H., Sung, K., Tashkun, S. A., Tennyson, J., Toth, R. A., Vandaele, A. C., and Vander Auwera, J.: The HITRAN 2008 molecular spectroscopic database, J. Quant. Spectrosc. Ra., 110, 533–572, 2009.

Sakabe, A., Kosugi, Y., Takahashi, K., Itoh, M., Kanazawa, A., Makita, N., Ataka, M.: One year of continuous measurements of soil CH_4 and CO_2 fluxes in a Japanese cypress forest: Temporal and spatial variations associated with Asian monsoon rainfall, J. Geophys. Res.-Biogeo., 120, 585–599, 2015.

Savage, K., Phillips, R., and Davidson, E.: High temporal frequency measurements of greenhouse gas emissions from soils, Biogeosciences, 11, 2709–2720, doi:10.5194/bg-11-2709-2014, 2014.

Schiller, C. L. and Hastie, D. R.: Nitrous oxide and methane fluxes from perturbed and unperturbed boreal forest sites in northern Ontario, J. Geophys. Res., 101, 22767–22774, 1996.

Schlesinger, W. H.: An estimate of the global sink for nitrous oxide in soils, Glob. Change Biol., 19, 2929–2931, 2013.

Seinfeld, J. H. and Pandis, S. mN.: Atmospheric Chemistry and Physics – From Air Pollution to Climate Change, 2nd Edn., John Wiley & Sons, Inc., Hoboken, New Jersey, 1232 pp., 2006.

Shurpali, N. J., Rannik, Ü., Jokinen, S., Lind, S., Biasi, C., Mammarella, I., Peltola, O., Pihlatie, M., Hyvönen, N., Räty, M., Haapanala, S., Zahniser, M., Virkajärvi, P., Vesala, T., and Martikainen, P. J.: Neglecting diurnal variations leads to uncertainties in terrestrial nitrous oxide emissions, Sci. Rep., 6, 25739, doi:10.1038/srep25739, 2016.

Skiba, U., Jones, S. K., Drewer, J., Helfter, C., Anderson, M., Dinsmore, K., McKenzie, R., Nemitz, E., and Sutton, M. A.: Comparison of soil greenhouse gas fluxes from extensive and intensive grazing in a temperate maritime climate, Biogeosciences, 10, 1231–1241, doi:10.5194/bg-10-1231-2013, 2013.

Thomson, A. J., Giannopoulos, G., Pretty, J., Baggs, E. M., and Richardson, D. J.: Biological sources and sinks of nitrous oxide and strategies to mitigate emissions, Philos. T. Roy. Soc. B, 367, 1157–1168, 2012.

Tuzson, B., Hiller, R. V., Zeyer, K., Eugster, W., Neftel, A., Ammann, C., and Emmenegger, L.: Field intercomparison of two optical analyzers for CH_4 eddy covariance flux measurements, Atmos. Meas. Tech., 3, 1519–1531, doi:10.5194/amt-3-1519-2010, 2010.

Wrage, N., Velthof, G. L., van Beusichem, M. L., and Oenema, O.: Role of nitrifier denitrification in the production of nitrous oxide, Soil Biol. Biochem., 33, 1723–1732, 2001.